TECHNICAL REPORT

STRUCTURAL SHELL OPTIMIZATION STUDIES

FINAL REPORT

FOUR VOLUMES

VOL. 4 EXPERIMENTAL BUCKLING TESTS OF MAGNESIUM MONOCOQUE ELLIPSOIDAL SHELLS SUBJECTED TO EXTERNAL HYDROSTATIC PRESSURE

BY

E. H. NICKELL

30 JUNE 1961

WORK DONE UNDER CONTRACT NOrd-18780(FBM), TASK III

Lockheed

MISSILES and SPACE DIVISION

LOCKHEED AIRCRAFT CORPORATION • SUNNYVALE, CALIF.

FOREWORD

This publication is the fourth of four volumes of the final report of an investigation of structural shell optimization. The present volume is a report of tests conducted on spun magnesium monocoque ellipsoidal shells subject to a uniform hydrostatic pressure.

The other three volumes of the final report have the following titles:

Vol. I	Survey of Buckling Data for Monocoque Circular Cylindrical Shells Subjected to Uniform External Pressure
Vol. II	Optimization of Stiffened Cylindrical Shells Subjected to Uniform External Hydrostatic Pressure
Vol. III	Influence Coefficients and Functions of Full-Tapered Conical Shells With Applications to Their Optimization Under Axial Loading

Included in this report is a design chart for predicting buckling pressure of Monocoque Ellipsoidal Shells.

The investigation was conducted by Structural Mechanics (L. A. Riedinger, Manager, Lockheed Missiles and Space Company) for the U. S. Navy Bureau of Weapons, Special Projects Office.

R. R. Johnson was Project Leader and R. F. Crawford was Technical Director for the work. Special acknowledgement is given to A. Holmes, Research Test Engineer, whose skill and active interest contributed significantly to the success of the investigation.

ABSTRACT

A design curve is presented for estimating the buckling pressure for Monocoque Ellipsoidal Shells subjected to an external hydrostatic pressure. This empirical estimation is based on test results from six Magnesium Ellipsoidal Shells with a major to minor radius ratio of three.

CONTENTS

Section		Page
	Foreword	ii
	Abstract	iii
	List of Illustrations	v
	List of Tables	vi
	Notation	vii
1	Introduction	1
2	Experimental Procedure and Results	2
3	Design Chart	25
4	Comparison of Estimates of Buckling Pressures	27
5	Problem Areas	29
6	Conclusions	30
7	References	32

ILLUSTRATIONS

Figure		Page
1	Comparison of Test and True Ellipsoidal Shell Geometry	3
2	Ellipsoidal Shell Before Failure	11
3	Failed Ellipsoidal Shell No. 1	12
4	Failed Ellipsoidal Shell No. 2	13
5	Failed Ellipsoidal Shell No. 3	14
6	Failed Ellipsoidal Shell No. 4 (External)	15
7	Failed Ellipsoidal Shell No. 4 (Internal)	16
8	Failed Ellipsoidal Shell No. 5	17
9	Failed Ellipsoidal Shell No. 6	18
10	Adjustable Test Jig End Plate for Ellipsoidal Shells	19
11	Assembled Ellipsoidal Shell End Plate	20
12	Strain Gage Locations	22
13	Actual Test Record of Strains	24
14	Comparison of Buckling Pressure of Ellipsoidal Shells With a Cylinder and Sphere	26
15	Design Chart	31

LIST OF TABLES

Table		Page
1	Thickness Measurements for Shell No 1	4
2	Thickness Measurements for Shell No 2	5
3	Thickness Measurements for Shell No 3	6
4	Thickness Measurements for Shell No 4	7
5	Thickness Measurements for Shell No 5	8
6	Thickness Measurements for Shell No 6	9
7	Ellipsoid" Shell Test Results	10

NOTATION

a = ellipsoidal shell depth (inches)

b = ellipsoidal shell-base radius (inches)

b_s = frame spacing (inches)

C_p = buckling coefficient

E = modulus of elasticity ($lb/in.^2$)

ℓ = truncated cone slant length (inches)

N_R = radius conversion factor

P_{cr} = critical buckling pressure (psi)

R = cylinder radius (inches)

R_1 = radius of small end of truncated cone (inches)

R_2 = radius of larger end of truncated cone (inches)

t = cone thickness (inches)

t_s = shell thickness (inches)

Δt = thickness increment (inches)

x, y = shell coordinates (inches)

Z = Batdorf's curvature parameter, defined by $Z = \sqrt{1 - \mu^2}\left(L/R\right)^2\left(R/t\right)$

Z_0 = curvature parameter for cone

μ = Poisson's ratio

α = semi-apex angle of cone

Section 1
INTRODUCTION

To satisfy performance requirements, high-speed aircraft and missiles require an aerodynamically shaped nose able to withstand high external pressures.

Designers and structural engineers must know critical buckling pressures of these shapes; they can be estimated by two known methods:

(1) Simplifying these shapes by cones, cylinders, or spheres, with equivalent geometry for which solutions– verified by tests– are available
(2) Testing the actual production aerodynamic shape

The first method results in a part likely to contain a considerable weight penalty; the second is valid for one shape only and is expensive and time consuming.

An empirical design chart whereby designers can improve their confidence in the initial design is part of this test program; results are reported herein.
Although the empirical design curve resulting from this program is limited, it is given as an interim method until theoretical solutions to this problem are solved.

Section 2
EXPERIMENTAL PROCEDURE AND RESULTS

The experimental results reported here are encouraging because high instability stresses with attendant weight savings are indicated for these shells of double curvature. The oversimplified analysis of these shapes, mentioned in the introduction, results in very conservative design or large weight penalties. This high strength of ellipsoidal shells may, in part, be attributed to the fact that the longitudinal compression tends to deflect the shell outward while the hoop compression tends to force the skin inward, resulting in a beneficial interaction. Tests of the ellipsoidal shells resulted in no scatter which is not typical of past buckling tests of thin shells of other shapes.

Six monocoque magnesium (AZ 31-B) ellipsoidal shells were tested. These shells were spun by Benson Manufacturing Co. of Kansas City, Missouri. The shells had three nominal thicknesses of 0.045, 0.065, and 0.087 inches. The shells have a modified ellipse shape as shown in Fig. 1, in which the test shape is compared with a true ellipse of equal major and minor axes. In each shell tested, the thickness varied considerably from the base to the apex. The thickness variations of each shell are recorded in Tables 1 through 6 for each 2-inch station along longitudinal lines in each quadrant. The average thickness in the tables was calculated from the thicknesses at the 12 longitudinal stations nearest the base of the shells. The observed critical buckling pressures are recorded in Table 7 and in photographs of each shell (Figs. 2 through 11). Shells 1, 2, 3, 4 and 5 were tested by pressurized air in a Bemco pressure chamber while shell No. 6 was tested first in the laboratory by evacuation. Shell No. 6 imploded violently; all of the other shells were then tested in an enclosed compartment. The bases of the shells were closed by an adjustable bulkhead designed and developed in LMSC's test laboratory. The bulkhead has an adjustable diameter and provides equal end support (almost simply supported) to each shell (Figs. 10 and 11).

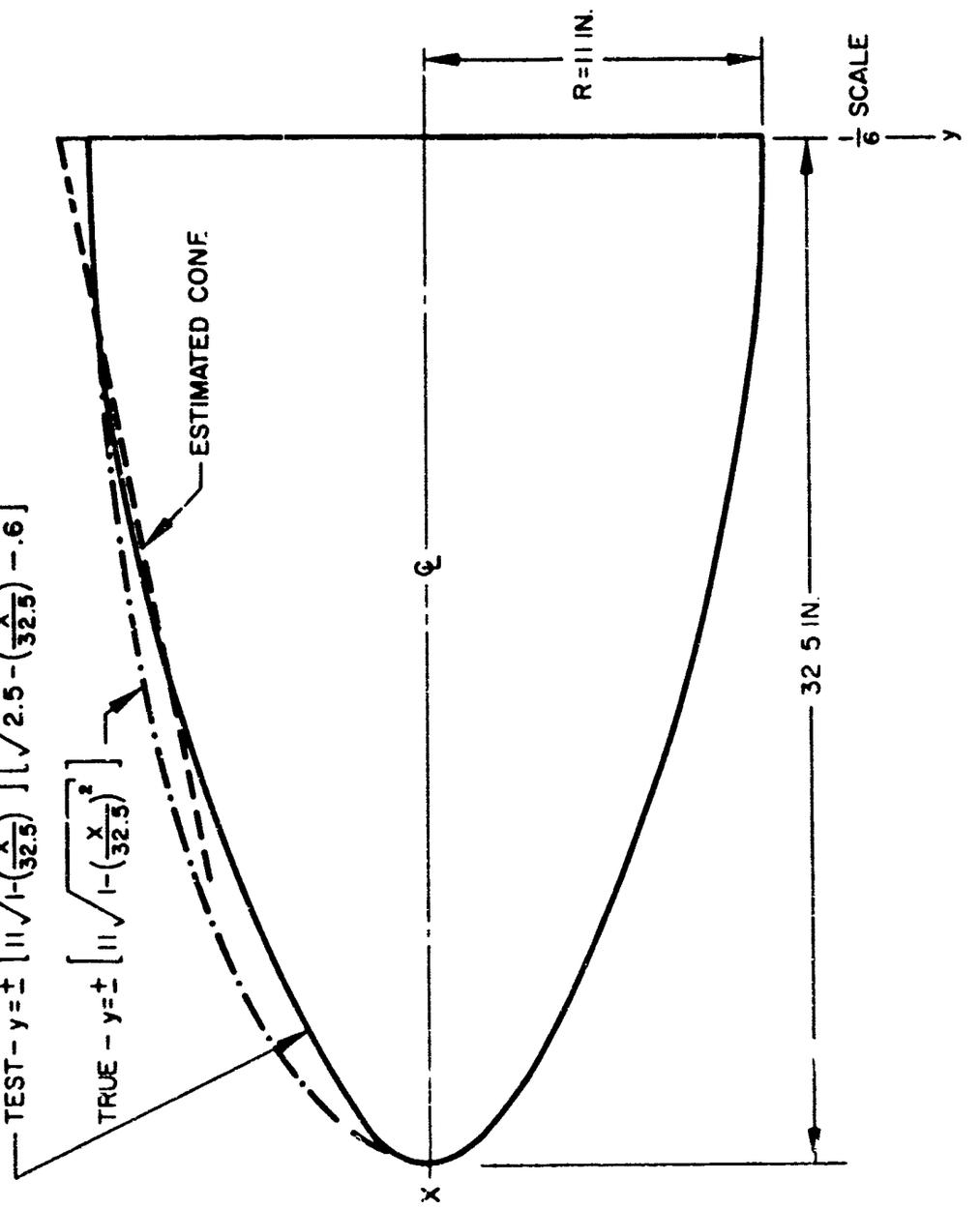

Fig. 1 Comparison of Test And True Ellipsoidal Shell Geometry

Table 1

SHELL THICKNESSES FOR SHELL NO. 1
(Inches)

Station	Quadrant			
	0°	90°	180°	270°
1	0.095	0.098	0.101	0.095
2	0.096	0.097	0.097	0.095
3	0.091	0.098	0.0905	0.092
4	0.093	0.093	0.093	0.092
5	0.092	0.092	0.092	0.0905
6	0.0935	0.0945	0.095	0.094
7	0.0935	0.0935	0.094	0.093
8	0.089	0.091	0.091	0.090
9	0.0865	0.0875	0.088	0.087
10	0.0865	0.0865	0.087	0.086
11	0.089	0.090	0.0895	0.087
12	0.089	0.089	0.089	0.088
13	0.080	0.081	0.080	0.081
14	0.085	0.086	0.085	0.0845
15	0.0845	0.085	0.085	0.085
16	0.0865	0.0875	0.087	0.0865
17	0.085	0.084	0.083	0.0825
Avg.	0.087	0.088	0.088	0.087

Table 2

SHELL THICKNESSES FOR SHELL NO. 2
(Inches)

Station	Quadrant			
	0°	90°	180°	270°
1	0.062	0.062	0.062	0.061
2	0.080	0.079	0.077	0.079
3	0.085	0.083	0.083	0.082
4	0.093	0.082	0.091	0.092
5	0.0955	0.095	0.0935	0.094
6	0.097	0.098	0.096	0.093
7	0.095	0.096	0.094	0.095
8	0.092	0.092	0.090	0.091
9	0.092	0.093	0.092	0.091
10	0.0885	0.090	0.087	0.089
11	0.090	0.092	0.090	0.091
12	0.090	0.090	0.088	0.090
13	0.082	0.086	0.080	0.085
14	0.082	0.088	0.077	0.084
15	0.080	0.084	0.079	0.081
16	0.087	0.090	0.088	0.088
17	0.082	0.082	0.076	0.083
Avg.	0.088	0.090	0.086	0.088

Table 3

SHELL THICKNESSES FOR SHELL NO. 3
(Inches)

Station	Quadrant			
	0°	90°	180°	270°
1	–	–	–	–
2	0.096	0.094	0.096	0.104
3	0.076	0.074	0.079	0.075
4	0.075	0.068	0.070	0.062
5	0.056	0.067	0.070	0.058
6	0.060	0.068	0.071	0.060
7	0.068	0.074	0.074	0.065
8	0.064	0.0715	0.070	0.063
9	0.068	0.0715	0.073	0.065
10	0.067	0.074	0.072	0.065
11	0.058	0.065	0.063	0.058
12	0.061	0.069	0.065	0.060
13	0.061	0.066	0.064	0.058
14	0.062	0.069	0.068	0.065
15	0.063	0.069	0.070	0.066
16	0.061	0.062	0.059	0.059
17	0.064	0.068	0.063	0.062
Avg.	0.063	0.069	0.068	0.062

Table 4

SHELL THICKNESSES FOR SHELL NO. 4
(Inches)

Station	Quadrant			
	0°	90°	180°	270°
1	0.052	0.055	0.058	0.049
2	0.057	0.060	0.058	0.058
3	0.055	0.055	0.054	0.054
4	0.056	0.056	0.055	0.056
5	0.052	0.053	0.051	0.051
6	0.049	0.048	0.049	0.048
7	0.046	0.045	0.048	0.047
8	0.037	0.038	0.041	0.039
9	0.041	0.038	0.037	0.039
10	0.047	0.048	0.046	0.045
11	0.046	0.044	0.048	0.044
12	0.044	0.043	0.043	0.042
13	0.045	0.044	0.042	0.041
14	0.045	0.046	0.048	0.044
15	0.048	0.045	0.046	0.045
16	0.046	0.045	0.047	0.042
17	0.050	0.048	0.049	0.048
Avg.	0.045	0.044	0.045	0.044

Table 5

SHELL THICKNESSES FOR SHELL NO. 5
(Inches)

Station	Quadrant			
	0°	90°	180°	270°
1	0.070	0.069	0.069	0.069
2	0.079	0.079	0.079	0.078
3	0.077	0.077	0.077	0.076
4	0.070	0.070	0.070	0.070
5	0.073	0.072	0.072	0.072
6	0.074	0.074	0.074	0.075
7	0.074	0.073	0.075	0.075
8	0.074	0.073	0.074	0.075
9	0.074	0.075	0.075	0.075
10	0.0645	0.066	0.067	0.067
11	0.069	0.069	0.070	0.069
12	0.062	0.070	0.068	0.067
13	0.061	0.068	0.064	0.063
14	0.065	0.070	0.065	0.065
15	0.067	0.072	0.068	0.076
16	0.073	0.070	0.073	0.070
17	0.069	0.068	0.069	0.067
Avg.	0.069	0.071	0.070	0.070

Table 6

SHELL THICKNESSES FOR SHELL NO. 6
(Inches)

Station	Quadrant			
	0°	90°	180°	270°
1	–	–	–	–
2	–	–	–	–
3	0.043	0.044	0.042	0.043
4	0.038	0.038	0.036	0.038
5	0.044	0.046	0.043	0.046
6	0.046	0.047	0.045	0.048
7	0.043	0.046	0.045	0.045
8	0.042	0.044	0.041	0.044
9	0.044	0.046	0.047	0.045
10	0.048	0.049	0.048	0.052
11	0.051	0.050	0.051	0.047
12	0.050	0.048	0.047	0.044
13	0.045	0.042	0.044	0.045
14	0.043	0.043	0.042	0.043
15	0.043	0.042	0.043	0.041
16	0.049	0.048	0.050	0.047
17	0.047	0.043	0.049	0.043
Avg.	0.046	0.046	0.046	0.045

Table 7

ELLIPSOIDAL SHELL TEST RESULTS

Shell Number	Average Thickness (Inches)	Buckling Pressure (psi)
1	0.087	46.1
2	0.087	47.0
3	0.065	28.0
4	0.045	13.5
5	0.070	31.9
6	0.045	13.8

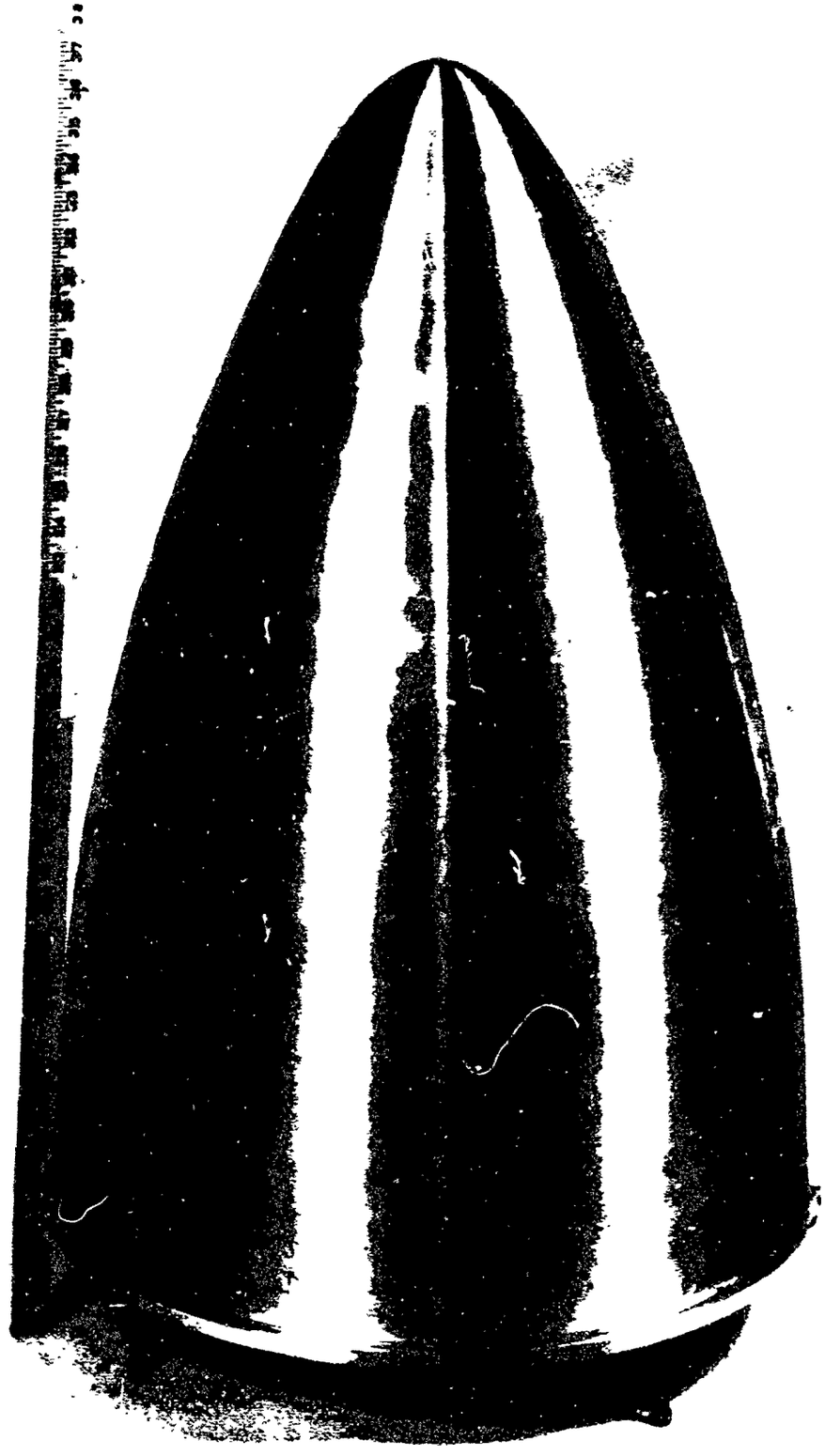

Fig. 2 Ellipsoidal Shell Before Testing With End Plate Attached

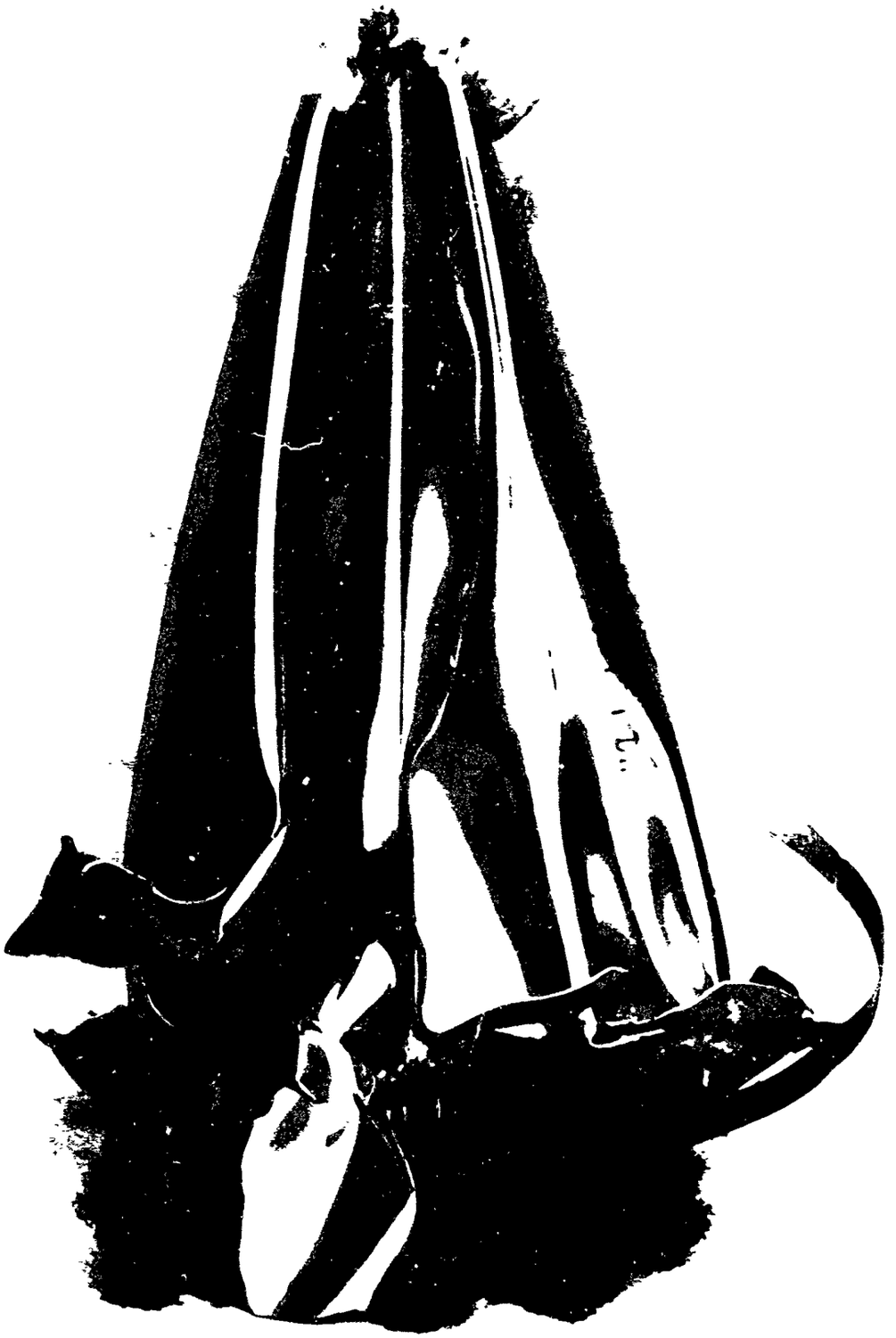

Fig. 3 Ellipsoidal Shell No. 1 (t_{avg} = 0.087 in. P_{cr} = 46.1 psi)

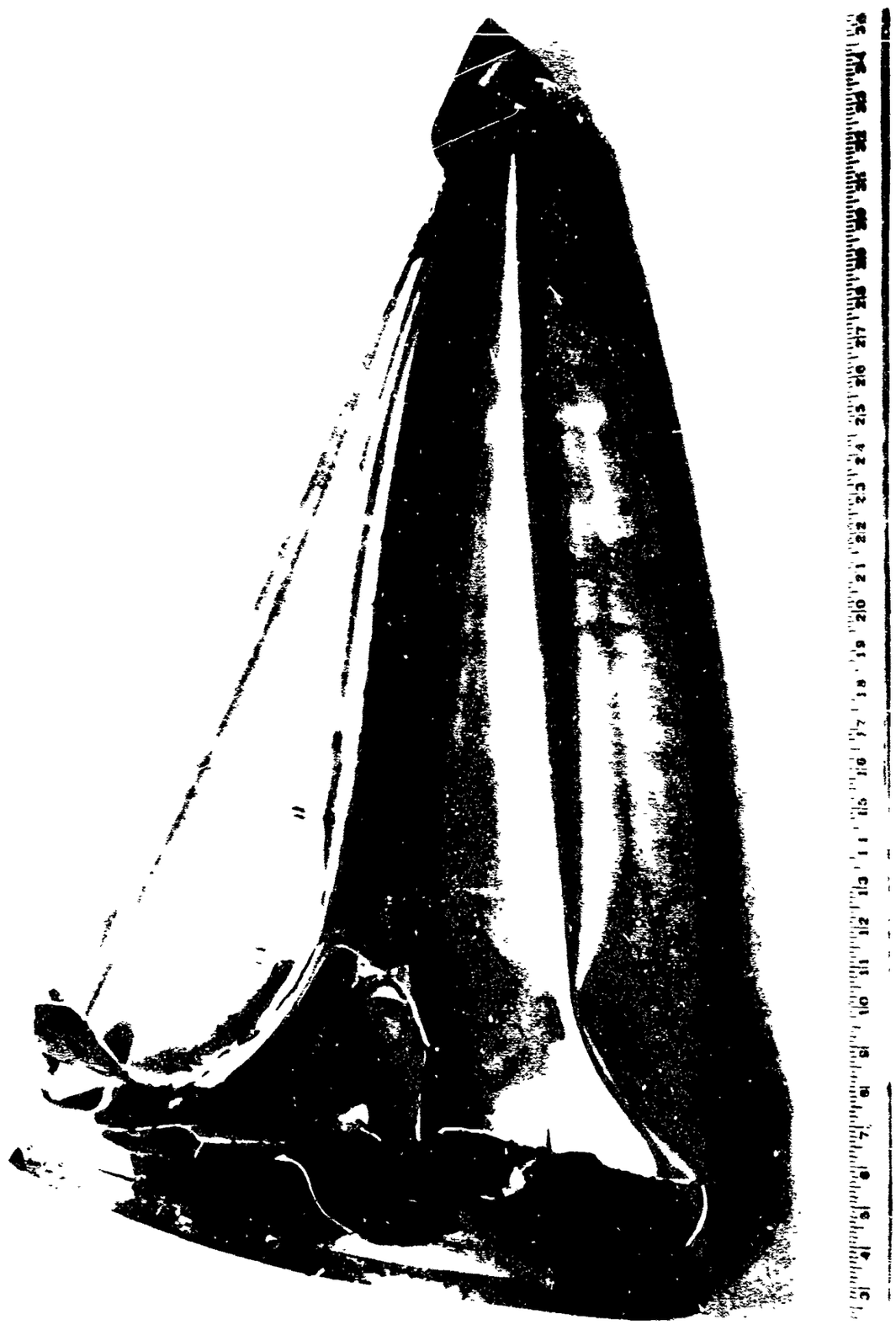

Fig. 4 Failed Ellipsoidal Shell No. 2 (t_{avg} = 0.087 in., P_{cr} = 47 psi)

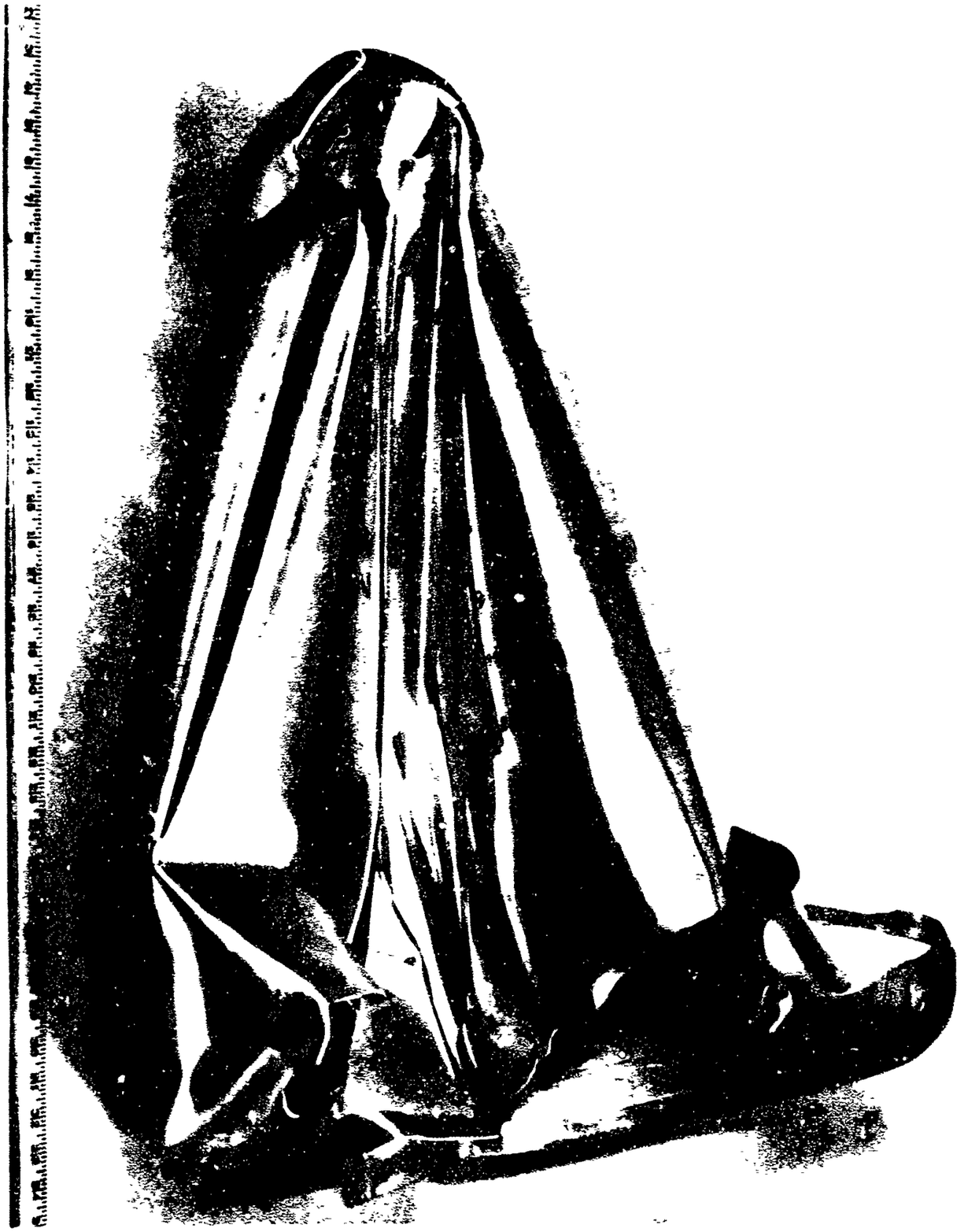

Fig. 5 Failed Ellipsoidal Shell No. 3 (t_{avg} = 0.065 in. P_{cr} = 28 psi)

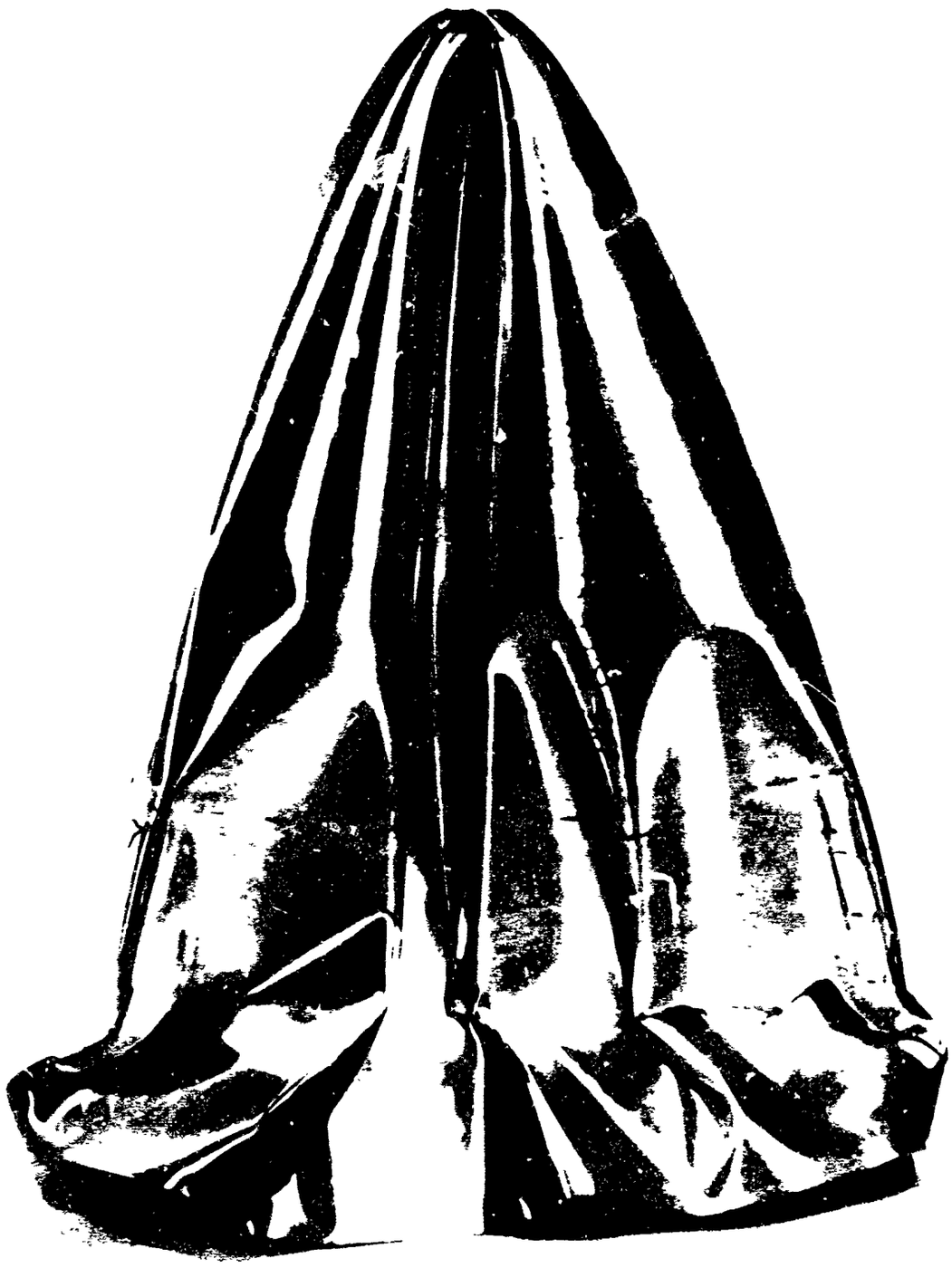

Fig. 6 Failed Ellipsoidal Shell No. 4 External (t_{avg} = 0.045 in. P_{cr} = 13.6 psi)

Fig. 7 Failed Ellipsoidal Shell No. 4 (t_{avg} = 0.045 in. P_{cr} = 13.1 psi)

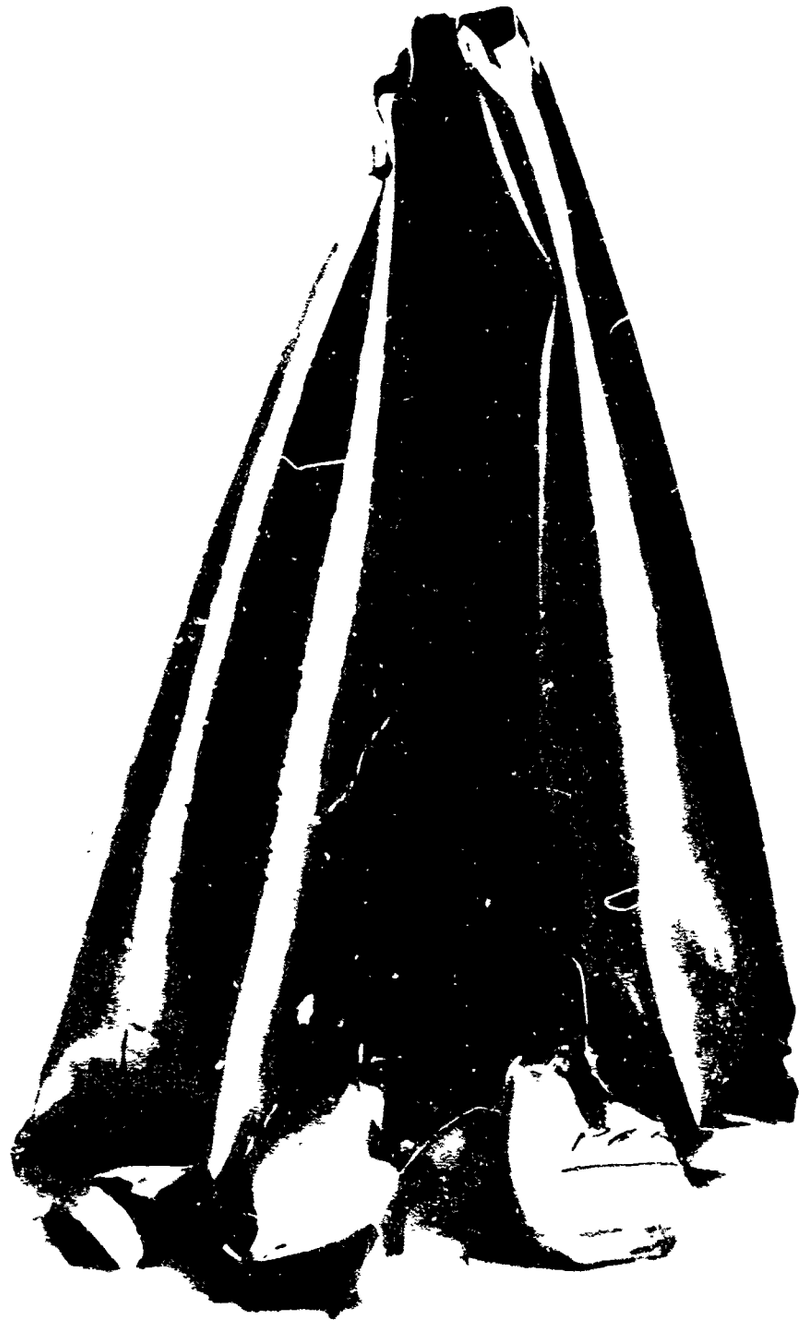

Fig. 8 Ellipsoidal Shell No. 5 (t_{avg} = 0.070 in. P_{cr} = 31 0 psi)

Fig. 9 Failed Ellipsoidal Shell No. 6 (t_{avg} = 0.045 in. P_{cr} = 13.8 psi)

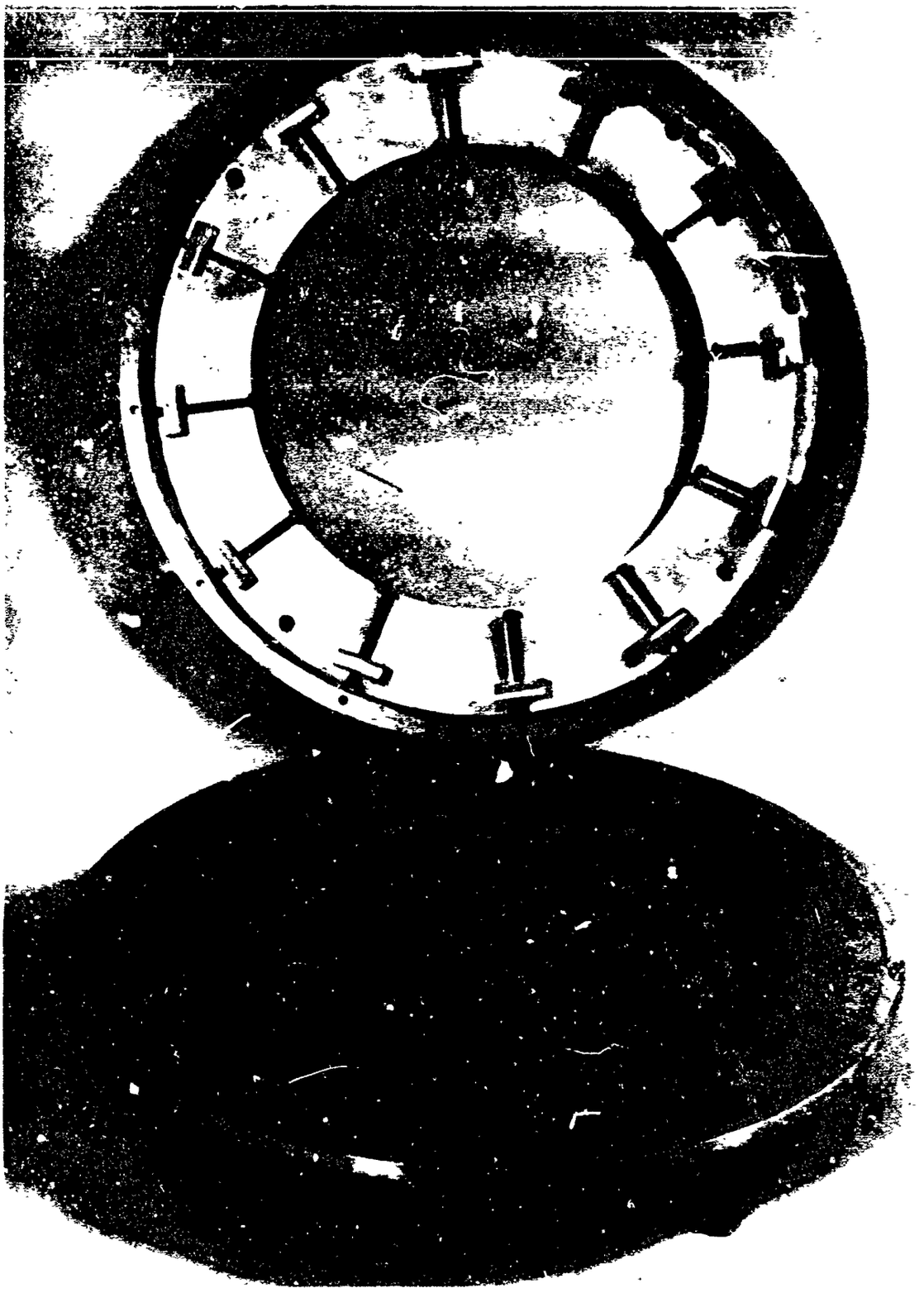

Fig. 10 Adjustable Test Jig End Plate for Ellipsoidal Shells

Fig. 11 Assembled Ellipsoidal Shell End Plate

Sheli No. 4 was instrumented to record prebuckling stress distributions. Twenty strain gages in pairs recorded bending stresses. These pairs were spaced equally around the circumference, 12 inches above the base as shown in Fig 12. The strains are recorded in Table 8. The actual test record is shown in Fig. 13. A plot of the prebuckling strains indicates four circumferential nodes.

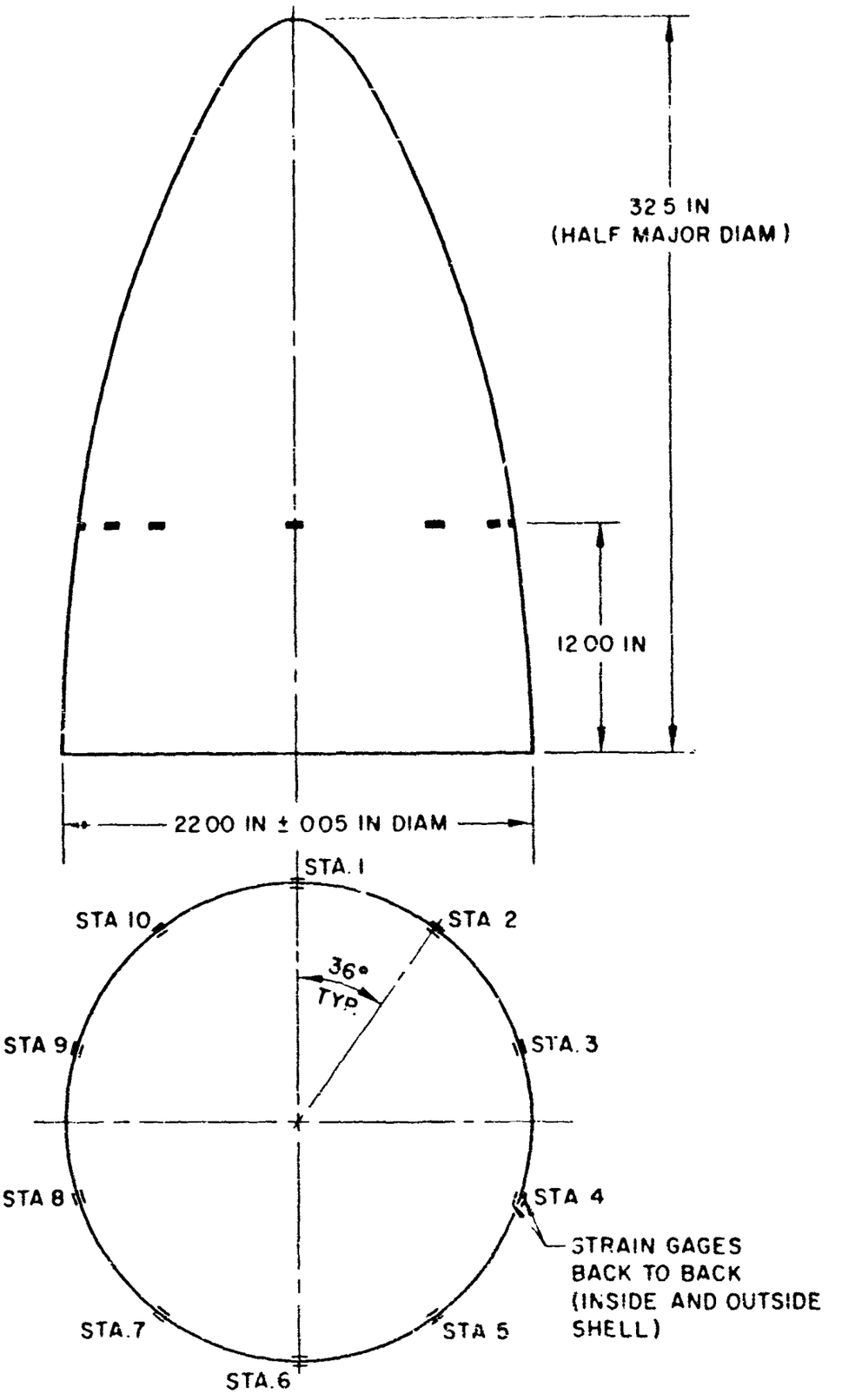

Fig. 12 Strain Gage Locations on Ellipsoidal Shell No. 4

Table 5

STRAIN READINGS OF ELLIPSOIDAL SHELL NO. 4

(Microstrain)

Differential Pressure	Station									
	1	2	3	4	5	6	7	8	9	10
(psi)										
+2	+2	-1	-3	0	-1	-5	0	+1	-1	0
0	—	—	—	—	—	—	—	—	—	—
12.50	68	2	38	66	30	12	-61	43	-19	-27
12.75	77	4	39	77	81	17	-63	55	-19	-38
13.00	87	4	42	93	104	22	-65	76	-21	-50
13.25	98	2	39	115	114	32	-65	109	-23	-76
13.50 Failure	115	0	36	142	172	42	-61	187	-25	-134

Positive bending tends to increase shell radius
Gage locations are shown in Fig. 12
Actual strain record is shown in Fig. 13

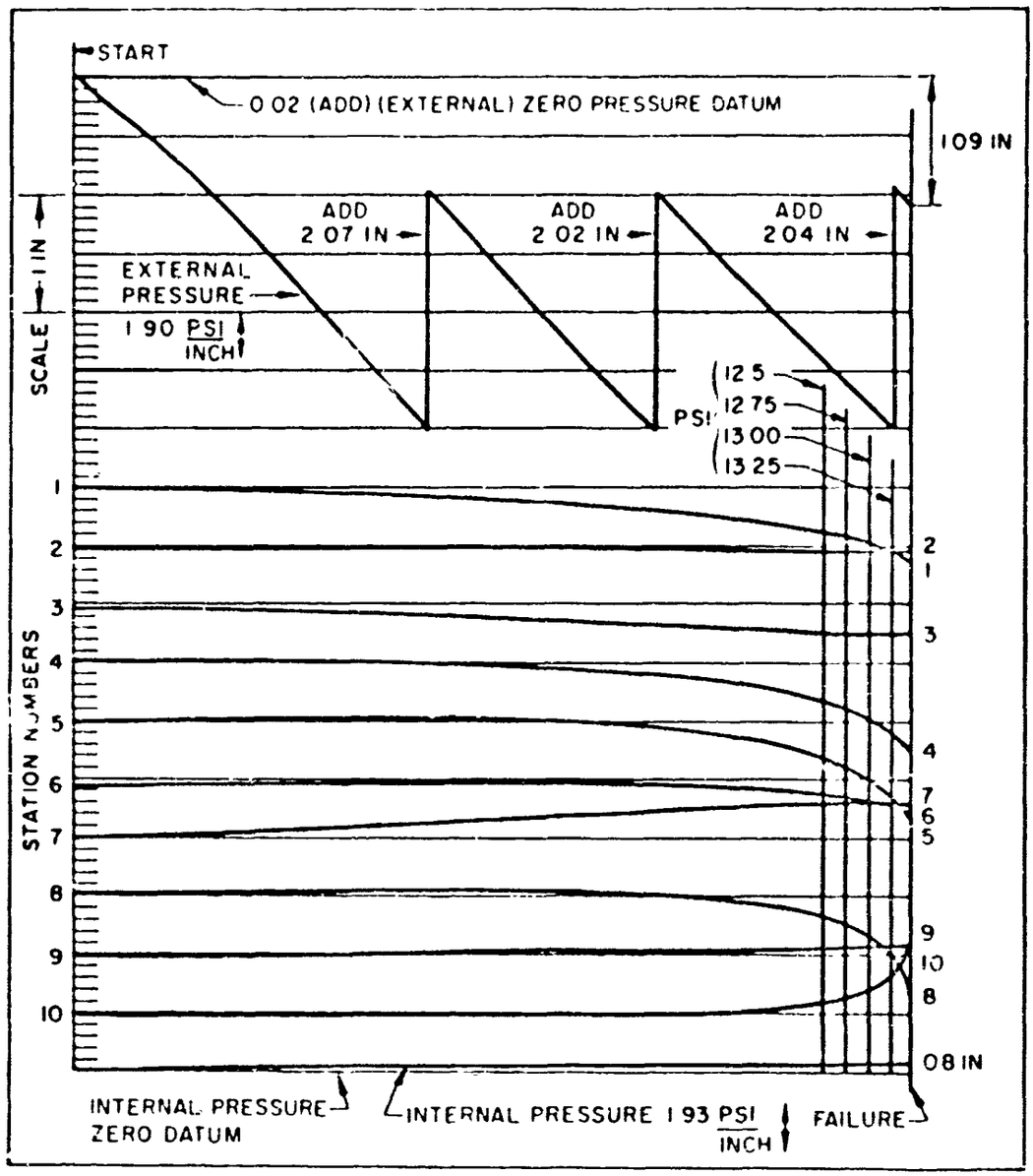

Fig. 13 Shell No. 4, Specimen No. 4 (0.045-in. Average Thickness), Failure Pressure, 13.5 psi. Tested 9 June 1961

Section 3
DESIGN CHART

The empirical design chart presented in Fig. 14 is a plot of the t_s/b versus P_{cr}/E curves for three ellipsoidal shells. These shells are the test shells with a major-to-minor radius ratio (a/b) equal to three. Included in Fig. 14 are two limiting cases of ellipsoidal shells: the infinitely long cylinder with an (a/b) ratio equal to ∞ and the sphere with an (a/b) ratio equal to one. The cylinder and sphere lines are theoretical curves from the classical small deflection solutions:

$$\text{Cylinder} - P_{cr}/E = \frac{1}{4\left(1 - \mu^2\right)} \left(\frac{t_s}{b}\right)^3 \tag{1}$$

$$\text{Sphere} - P_{cr}/E = \frac{2}{\sqrt{3\left(1 - \mu^2\right)}} \left(\frac{t_s}{b}\right)^2 \tag{2}$$

The tests plotted on Fig. 14 resulted in a straight line with a slope of two, which is the same slope as the sphere. The equation of the line for the test points is:

$$\frac{P_{cr}}{E} = \frac{1}{12\left(1 - \mu^2\right)} \left(\frac{t_s}{b}\right)^2 \tag{3}$$

The assumption that Poisson's Ratio μ is equal to three tenths permits the equation(s) to be written similar to Eqs. (1) and (2).

To estimate the buckling pressure for shells with other a/b ratios, a crossplot of Fig. 14 is made holding t_s/b constant and estimating a curve between the three points with ordinate a/b and abscissa P_{cr}/E. For various t_s/b ratios, then, a family of t_s/b curves as shown in Fig. 15 results. From this design chart, the critical pressures may be estimated for any a/b ratio. Obviously, additional tests would be helpful in more precisely defining the shape of these curves between $\infty > a/b > 3$.

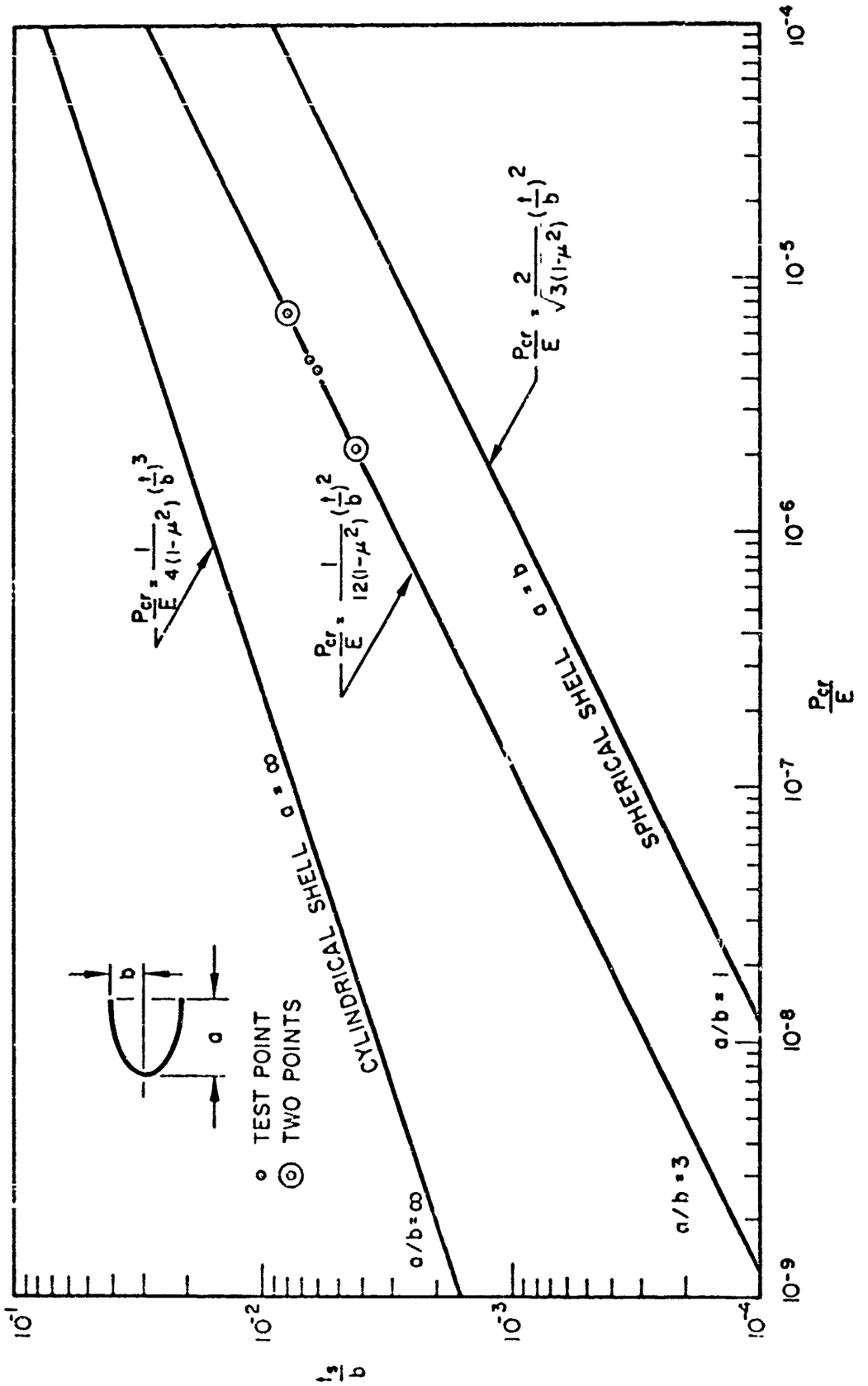

Fig 14 Comparison of Hydrostatic Buckling Pressure Tests of Ellipsoidal Shells With Cylinder and Sphere

Section 4
COMPARISON OF ESTIMATES OF BUCKLING PRESSURES

An example comparison of a prediction between buckling pressure based on conical shell analogy and the observed test results is made. This comparison best shows the advantage of double curvature shells and the inadequacy of resorting to such analogy methods.

A somewhat similar conical shell is chosen as being structurally as well as geometrically analogous to the shell shape shown by the small dotted line in Fig. 1. The analogous cone has the following geometry.

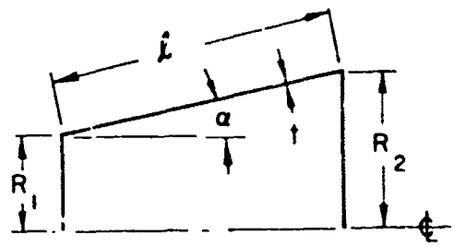

$t = 0.045$ in. $\quad \alpha = 11.5$ deg

$R_2 = 12$ in. $\quad \ell = 20$ in.

$R_1 = 7$ in.

The critical buckling pressure is calculated by using the method (Ref. 1) which determines a cylinder structurally equivalent to the cone. A buckling pressure for the

equivalent cylinder is calculated as

$$Z_o = 0.954 \left(\frac{\ell}{R_2}\right)^2 \left(\frac{R_2}{t}\right) \cos \alpha = 692$$

$$\mathcal{N}_R = 0.77$$

$$\frac{R}{t} = \frac{\mathcal{N}_R}{\cos \alpha} \left(\frac{R_2}{t}\right) = 210$$

$$Z = Z_o/\mathcal{N}_R = 898$$

$$C_p = 32.5$$

$$P_{cr} = C_p (0.904) \frac{E}{Z (R/t)^2} = \underline{\underline{4.83}} \text{ psi}$$

The actual buckling pressures for shells No. 4 and No. 6 were 13.5 and 13.8 psi, respectively, which is 3-1/2 times the estimated 4.83 psi calculated above. Since the geometrically similar conical shell is shown not to be structurally analogous, then use of such methods of predicting critical pressures is to be avoided.

Section 5

PROBLEM AREAS

Until a theoretical buckling analysis is derived for ellipsoidal shells, additional testing will be necessary to verify designs based on the design chart submitted in this report. More substantiation or refinement (either theoretical or experimental)of these design charts is needed before the apparently high efficiencies of double curved shells may be realized. Further, the effects of stiffeners on double curved shells should be determined for possibly increased efficiency. An initial effort in this area which offers considerable potential weight savings would be to experimentally evaluate the effects of rings to reduce the natural longitudinal buckle wave lengths and thereby increase critical pressure.

Section 6
CONCLUSIONS

An estimate of buckling pressures for Monocoque Ellipsoidal Shells can be made with the use of the design chart (Fig. 15) for various major-to-minor radius (a/b) ratios. The test results included give critical buckling pressures for six Monocoque Magnesium Modified Ellipsoidal Shells. Prebuckling stress distributions are given for one shell.

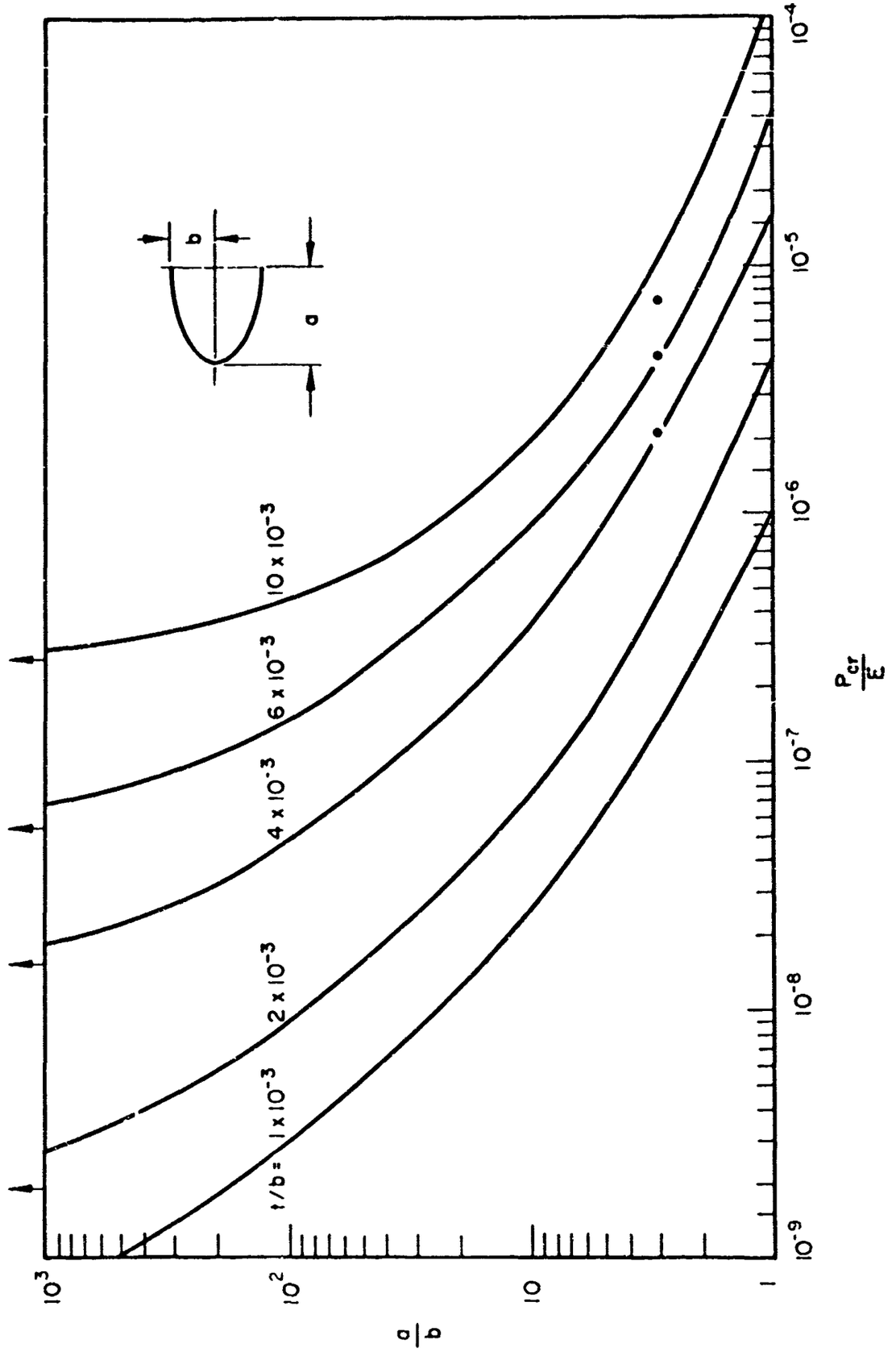

Fig. 15 Hydrostatic Buckling Pressure for Ellipsoidal Shells versus a/b ratios

Section 7
REFERENCES

1. E. V. Pittner and F. G. Morton, "A Method of Analysis for Buckling of Monocoque Conical Shells Subjected to Hydrostatic Pressure," Vol. 11 of Final Report on Stress and Stability Analysis of Cylindrical and Conical Shells, LMSD-894808, Sunnyvale, Calif. 30 June 1961 (U)